Estimations of the Shielding Requierements for the Neutron Beam Line of the NSE Instrument at SNS and a First Engineering Design

—DRAFT—

K. Nünighoff
Institut für Kernphysik, Forschungszentrum Jülich GmbH, D-52425 Jülich, Germany

M. Monkenbusch, M. Ohl, T. Kozielewski
Institut für Festkörperforschung, Forschungszentrum Jülich GmbH, D-52425 Jülich, Germany

M. Butzek
Zentralabteilung Technologie, Forschungszentrum Jülich GmbH, D-52425 Jülich, Germany

25th July 2004

1 Introduction

In this report the results of the radiation shielding calculations for the **N**eutron-**S**pin-**E**cho Instrument (NSE) are described. This Instrument will be constructed at beam line 15. The aim of this study was the determination of the necessary thickness and length of the radiation shielding to achieve the requiered dose rate limit of 0.25 mrem/h at the surface of the shielding. The influence of different materials, like regular concrete, high density concrete, steel, and tungsten was investigated. The dose rate was entangled for neutrons and γ-rays for the following energy regions:

- neutrons
  - thermal neutrons E_{kin} <1.12 eV
  - epithermal neutrons 1.12 eV < E_{kin} < 1.11 MeV
  - fast neutrons 1.11 MeV < E_{kin} < 19.6 MeV
  - very fast neutrons fast neutrons 19.6 MeV < E_{kin} < 1 GeV
- γ-rays
  - low energy γ-rays E_{kin} <1 MeV
  - high energy γ-rays 1 MeV < E_{kin} < 20 MeV

This study showed, that on the one hand the dose rate due to the γ-flux is up to a factor of ten lower than the dose rate caused by the neutron flux, and on the other hand, that the dose rate is dominated by the high energy neutron flux above E_{kin} >20 MeV. The effectiveness of high density concrete to reduce the dose rate led to the decision to use this material for the shielding in spite of the high costs. The presented results led to a first engineering design of the beamline shielding, which is presented in Sec. 9.

2 Methode of Calculation

To determine the dose rate the methode of discrete ordninates was chosen, i.e. a numerical solution of the Boltzmann transport equation. Because this estimations are urgent needed for starting the mechanical design of the beam line shielding, the approach of a Monte-Carlo simulation with e.g. MCNPX [1] was not taken into account. To determine the needed thicknesses of the shielding, two dimensional SN-calculations with the DORT code [2] were performed. For this reason the geometry of the neutron beamline was simplified as a r-z-geometry based on concentric cylinders. The source term –provided by the SNS– describes the neutron energy spectrum on the moderator surface (A≈400 cm^2) entering a 25° cone and was calculated with MCNPX using a detailed geometric description of the SNS target-moderator-reflector assembly [3]. In all described calculations the source term was normalized to the

cross section of the neutron guide of 32 cm^2, i.e. a reduction of the initial neutron flux by a factor of 0.08. With the GRTUNCL code a first collision source was generated and used as a source term for the DORT calculations.
The DORT calculations are perfomed in two steps, because the neutron beam line is bended at a distance of 5.90 m from the moderator surface. At this position a Si-bender changes the direction of the thermal and cold neutrons by 3.5°, preventing high energy neutrons directly travelling to the instrument. During the first step the isodose plot of the shielding surrounding the beam line in 0°-direction is generated. After that the angular and directional fluxes are combined and transformed to the 3.5°-dircection starting at the midpoint of the Si-bender. With this flux distribution the isodose plot of the bended beam line was generated. Due to the described methode the flux of thermal and cold neutrons travelling through the bender and the neutron guide is underestimated, because the neutron optic properties of the neutron guide as well as bender is not taken into account. This means that the contribution of thermal neutrons to the dose rate is underestimated.

3 Used Parameters

For all calculations the P5 Legendre scattering order and the U 100 upward bias quadrature set was used. The cross sections were taken from the HILO-2K library [5] with 83 neutron groups and 22 γ-groups. The cross sections used in the DORT calculations are processed with the AXMIX code [6] and the GIP code [7]. In Tab. 1 the material mixtures and used nuclear densities are listed. The data for selected materials like stainless steel and concrete are taken from a SNS report [8].

4 DORT Model of the neutron beamline

To perfom the DORT calculations with a r-z-cylinder geometry the geometry of the neutron beamline was simplified. The rectangular cross section of the neutron guide (4 cm x 8 cm) was simplified as a cylinder with the same cross section area, i.e. a radius of 3.2 cm. This vacuum tube is surrounded with a 1.5 cm thick layer of boron glas. Between the boron glas and the 5 cm thick iron support structure of the neutron guide is a 0.5 cm air gap. Between the support structure and the outer shielding materials a further gap of 1 cm is included in the calculational model. The neutron guide ends in the 0°-direction at 6.70 m. The first 5 m of the neutron guide is surrounded with stainless steel, representing the shielding monolith of the target station. In the 0°-direction between 5 m and 11 m high density concrete is used as shielding material. Four choppers are planed for this instrument. In the DORT model the choppers are simpliefied as void cylinders with a radius of 51.2 cm and a length of 40 cm. These chopper cavities are located at distances from the moderator surface of 5.20 m, 6.30 m, 7.90 m, and 10.10 m. Between the first two choppers the revolver system is located. It contains different benders, which are positioned at a distance of 5.90 m (midpoint of the bender) from the moderator surface. The length of this device is 70 cm and the diameter is 1.2 m. As material stainless steel was used. The bender is modeled as a pure silicon cylinder with a radius of 3.2 cm and a length of 10 cm. Fig. 1 illustrates the geometry model of the 0°-direction. The radius of this geoemtry is 2.26 m. The beam axis of the bended part of the neutron beamline starts at the midpoint of the silicon bender at a distance of 5.90 m from the moderator surface and the deflection is 3.5°. In this part the last three choppers are included. Whereas up to 10 m the shielding is made of high density concrete, the last meter is made of normal concrete to avoid influences of the magnetic field at the sample position due to the ferromagnetic properties of the iron composites of the high density concrete. For large distances of 11 m from the moderator surface the neutron guide is surrounded by air. The radius of this part is 1.26 m. A plot of the geometry of the 3.5°-direction is also shown in Fig. 1. The green areas represent zones in the geometry for a beamstop in order to reduce the dose rate in axial direction. The influence of the beamstop will be discussed later in section 5.

Material	Element	nuclear density
normal concrete	hydrogen	$7.76555 \cdot 10^{-3}$
	oxygen	$4.38499 \cdot 10^{-2}$
	sodium	$1.04778 \cdot 10^{-3}$
	manganese	$1.48662 \cdot 10^{-4}$
	aluminium	$2.38815 \cdot 10^{-3}$
	silicon	$1.58026 \cdot 10^{-2}$
	sulfur	$5.63433 \cdot 10^{-5}$
	potassium	$6.93104 \cdot 10^{-4}$
	calcium	$2.91501 \cdot 10^{-3}$
	iron	$3.05275 \cdot 10^{-4}$
dry air	nitrogen	$4.2 \cdot 10^{-5}$
	oxygen	$9.6 \cdot 10^{-6}$
pure silicon	silicon	$5.01200 \cdot 10^{-2}$
borofloat glas	boron (^{10}B)	$7.19865 \cdot 10^{-4}$
	boron (^{11}B)	$2.63414 \cdot 10^{-3}$
	oxygen	$4.61287 \cdot 10^{-2}$
	sodium	$1.70529 \cdot 10^{-3}$
	aluminium	$2.65012 \cdot 10^{-4}$
	silicon	$1.80161 \cdot 10^{-2}$
high density concrete	hydrogen	$2.43639 \cdot 10^{-1}$
	oxygene	$8.24233 \cdot 10^{-2}$
	sodium	$1.23498 \cdot 10^{-5}$
	magnesium	$6.80524 \cdot 10^{-5}$
	aluminium	$2.32759 \cdot 10^{-4}$
	silicon	$4.82175 \cdot 10^{-4}$
	sulfur	$1.63072 \cdot 10^{-3}$
	potassium	$1.89363 \cdot 10^{-5}$
	calcium	$8.49706 \cdot 10^{-6}$
	manganese	$1.82854 \cdot 10^{-3}$
	iron	$1.18462 \cdot 10^{-2}$
void	hydrogen	0.0
stainless steel	carbon	$3.22431 \cdot 10^{-4}$
	silicon	$1.80504 \cdot 10^{-3}$
	chromium	$1.58115 \cdot 10^{-2}$
	manganese	$1.75872 \cdot 10^{-3}$
	iron	$5.64615 \cdot 10^{-2}$
	nickel	$1.18862 \cdot 10^{-2}$

Table 1: Materials and compositions used in DORT calculations.

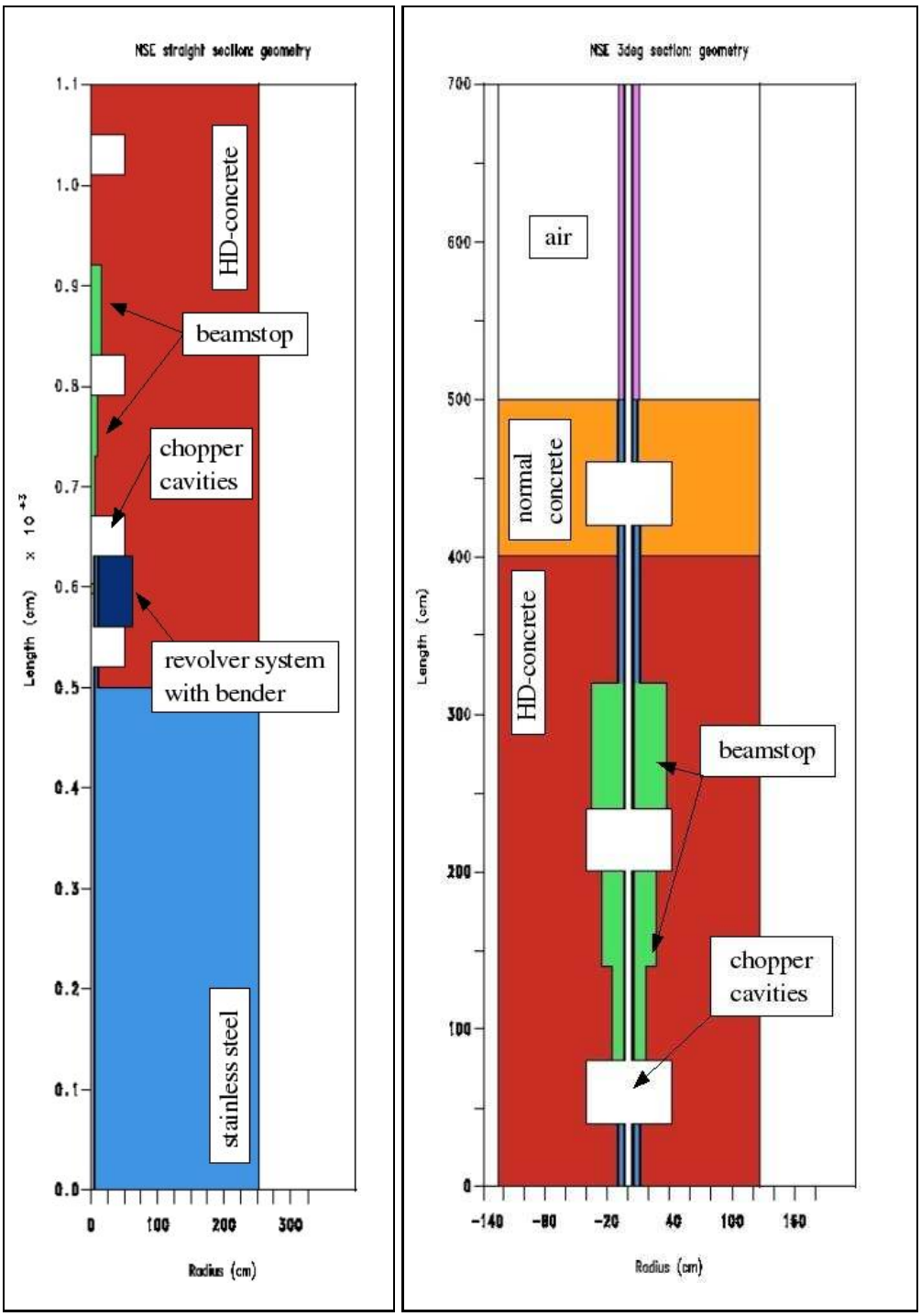

Figure 1: 2D-r-z-geometry model of the 0°-direction (left picture) and of the 3.5°-direction (right picture) of neutron beam line of the NSE instrument.

5 Beamline Shielding in 0°-direction

In the first step the dose rates caused by neutrons and gammas were calculated for the 0°-direction. In Fig. 2 the isodose plots for gamma, neutron, and the total dose rate (n+γ) are shown. It can be seen that the γ-radiation plays a minor role and that the total dose rate is dominated by neutrons. The distribution of the dose rate on beam axis is shown in Fig.4. It can be seen that the required dose rate limit of 0.25 mrem/h is met in a distance of 9.3 m from the moderator surface.

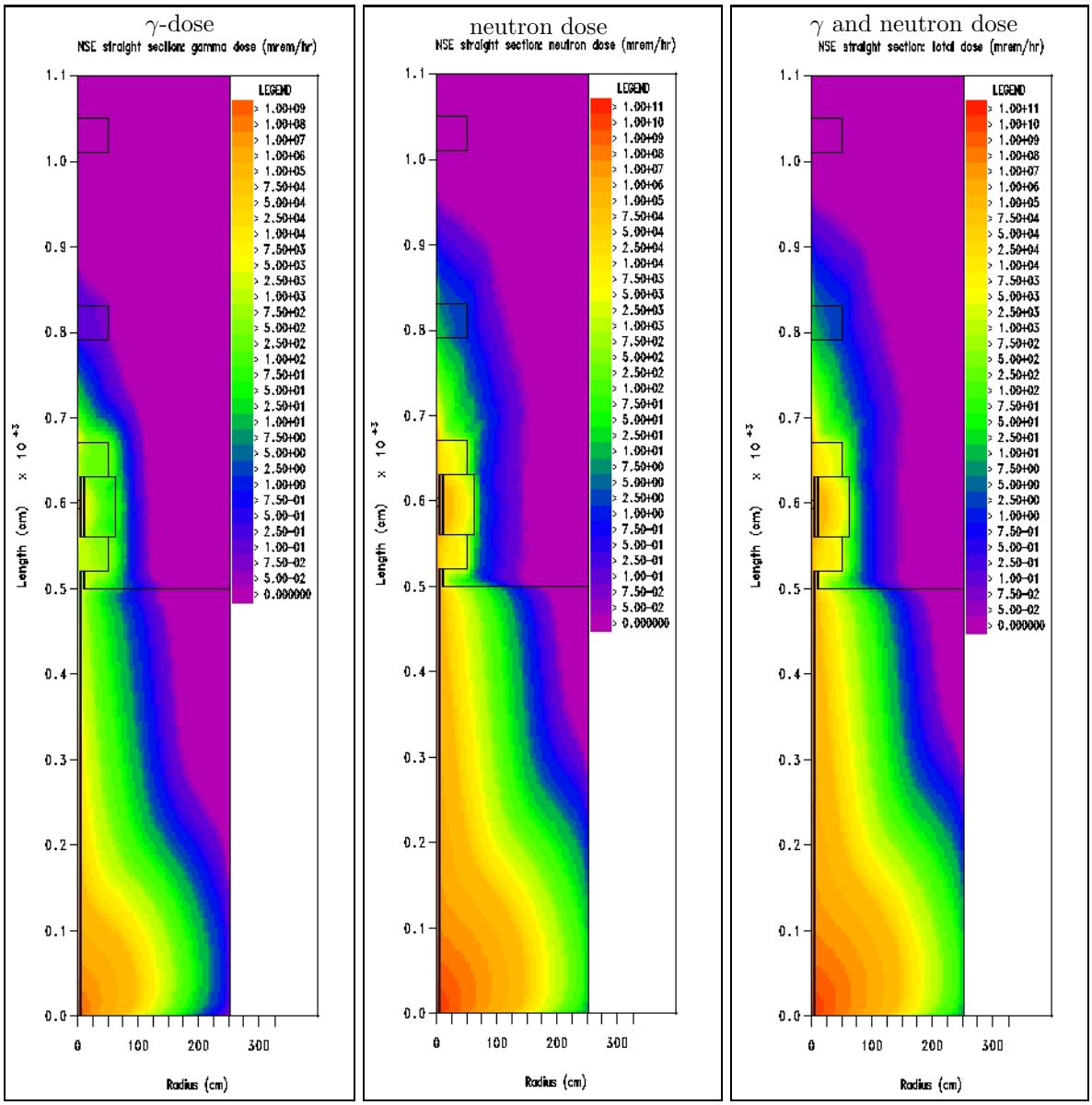

Figure 2: *Isodose plot for γ-, n-, and γ+n-radiation in 0°-direction.*

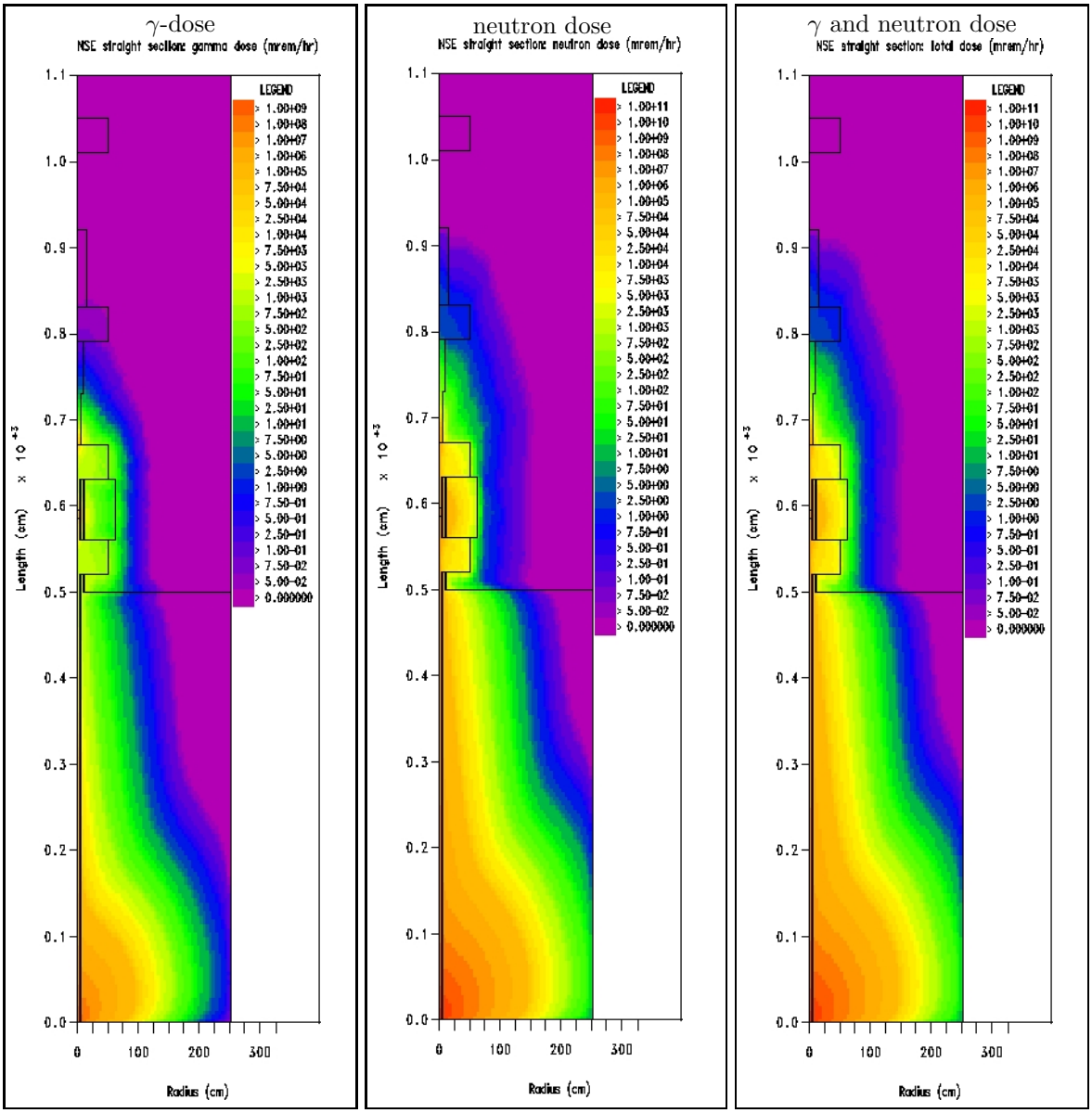

Figure 3: *Same as Fig. 2, but with a stainless steel beamstop.*

In order to reduce the dose rate the influence of a stainless steel beamstop was investigated. This beamstop consist of three parst. The first part starts at z=6.7 m and ends at z=7.3 m and has a diameter of 10.4 cm. The second part starts directly behind the first part and has a length of 0.6 m and a diameter of 20.4 cm. The third part is located behind the third chopper and has length of 80 cm and a diameter of 32.4 cm. Whereas in the 0°-direction the beam stop replaces the neutron guide, in case of the 3.5°-direction the beamstop surrounds the neutron guide with the same outer radii. The position of the beam stop can be seen in Fig. 1. The resulting isodose plots are shown in Fig. 3. The main result is, that the dose rate in radial direction is not influenced by the beamstop and that the dose rate in direction of the primary neutron beam is slightly reduced. The dose rate limit of 0.25 mrem/h is already met at a distance of 9 m instead of 9.30 m (see left picture in Fig. 4) without the stainless steel beamstop. From the radiation shielding point of view the advantage of the stainless steel beamstop is negligible. However, from the desing layout it is much more complicated to construct a beamline shielding with concrete blocks close to the neutron guide.

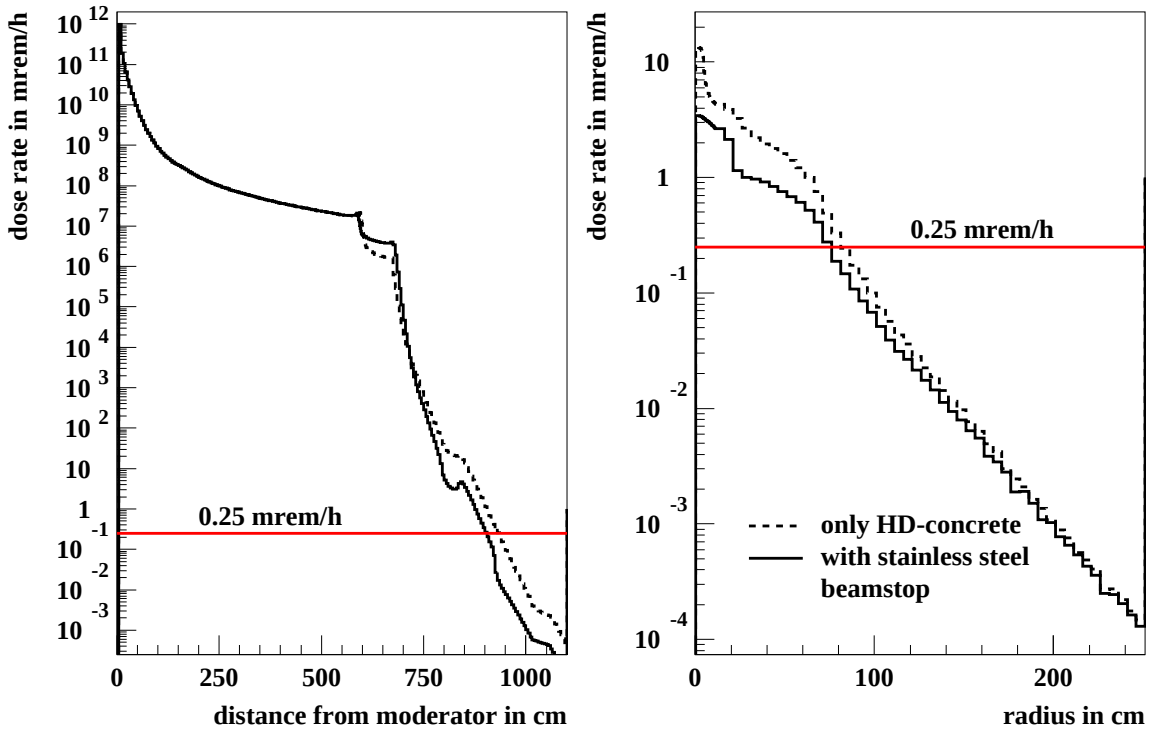

Figure 4: The left picture shows the dose rate on the z-axis with and without a stainless steel beamstop. The right picture shows the same, but perpendicular to the beam axis in a distance of 8 m from the moderator surface.

The left picture in Fig. 4 shows the dose rate as a function of the distance from the moderator. Up to ≈6 m the dose rate shows the expected $1/r^2$ dependency. The change of slope due to the material change at the bender position (5.90 m) as well as at the beginning of the beamstop at 6.7 m can be seen. The two plateaus at 5.4 m, 6.5 m, and 8.1 m are caused by the chopper cavities. The small advantage of the stainless steel beamstop can also be seen in this figure. The right picture in Fig. 4 shows the radial dependency of the dose rate at a distance from the moderator of 8.5 m. It can be seen, that the dose rate in radial direction can be reduced by the stainless steel beamstop. But the effect can only be observed for a radius less than 0.7 m. From this result it can be concluded, that a reduction of the needed thickness of the radiation shielding in radial direction cannot be achieved with a stainless steel beamstop.

5.1 Radial Dependency of the dose rate

In Fig. 5 the dose rate as a function of the radius is shown for four selected axial position: at 5.40 m (first chopper cavity), 5.90 m (midpoint Si-bender), 6.50 m (second chopper cavity), and 8.50 m (stainless steel beamstop). In this figure the influence of different materials in radial direction can be seen. At

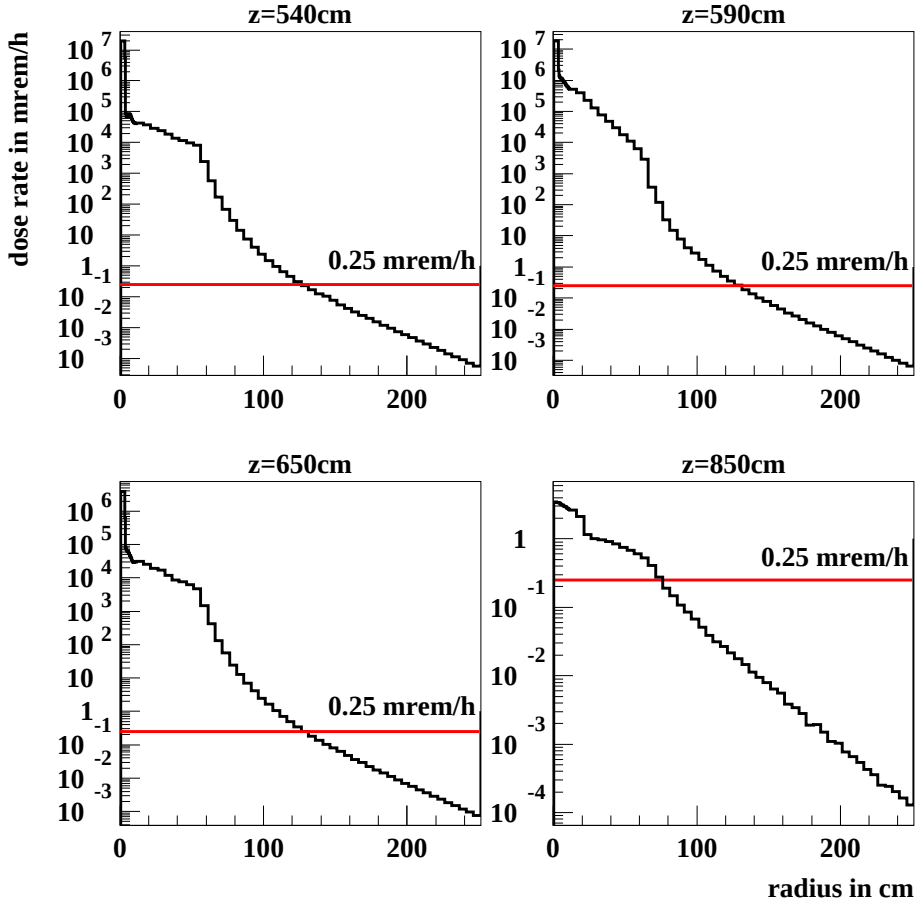

Figure 5: Radial dependency of the dose rate at selected axial positions. The red line marks the dose rate limit of 0.25 mrem/h.

z=5.4 m and z=6.5 m the plateau between 10 cm and 50 cm is due to the first and second chopper cavity, which is modeled as a void cavity. Above a radius of 51.2 cm the decrease of the dose rate due to the HD-concrete shielding can clearly be seen. In the histogram for z=5.9 m the change from the stainless steel cylinder of the revolver system to the HD-concrete shielding can be observed as a change of the slope of the histogram at a radius of 60 cm. At z=8.5 m an edge at a radius of 20 cm can be observed. This edge marks the border between the stainless steel beamstop and the HD-concrete shielding. An estimation of the required thickness of the shielding as a function of the beam line length can be found in sect. 6.3.

6 Shielding of the 3.5°-direction

In the second step of the calculations the spatial dose rate distribution of the bended beam line was investigated. Two main question have to be answered:

- Is the isodose distribution influenced by the bender length?
- Which length of the shielding is required?

In the following subsections answers to this question will be given.

6.1 Influence of the Length of the Si-Bender

In this section the influence of different lengths of the Si-bender on the spatial distribution of the dose rate will be discussed. The revolver system will contain three benders and an auxiliary beamstop. The benders have lengths of 2 cm, 10 cm, and 20 cm. The midpoint of all three benders is at 5.90 m. In Fig. 6 the dose rate on the beam axis of the 0°-direction is shown. Behind the bender the dose rate

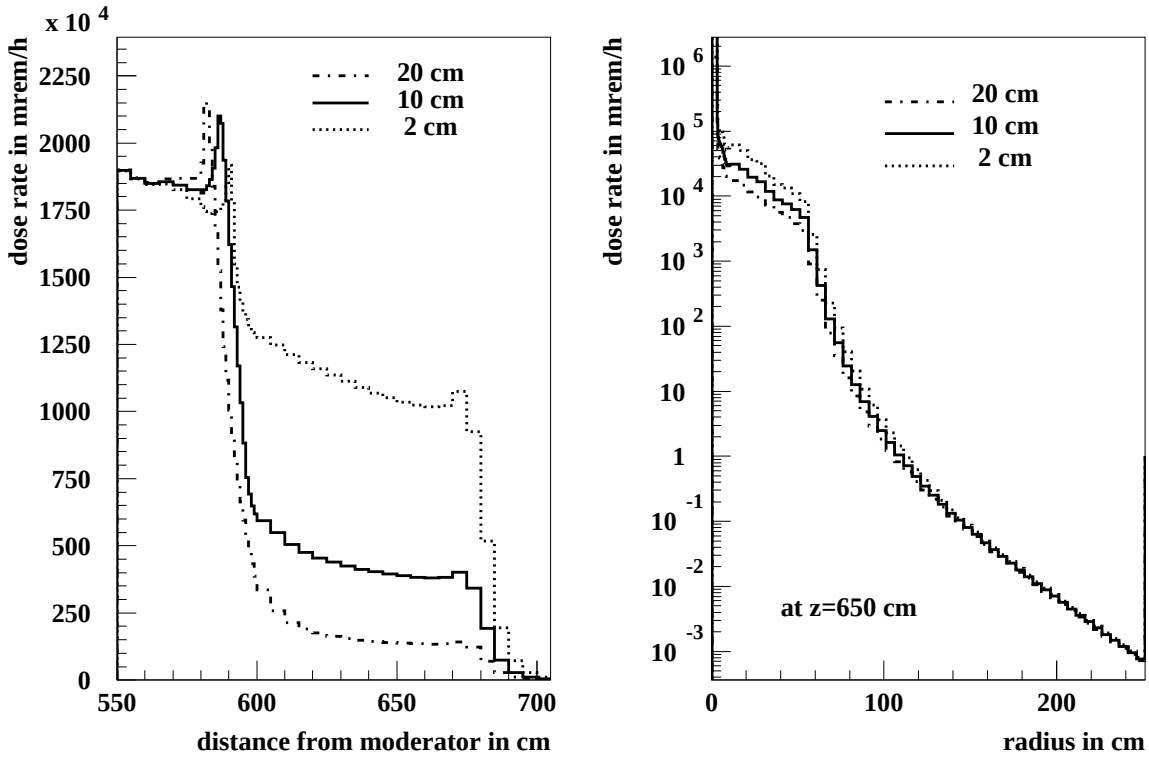

Figure 6: Dose rate on beam axis in 0°-direction (left picture) and the as a function of the radius at z=650 cm (right picture) for three different bender lengths of 2 cm, 10 cm, and 20 cm.

shows an expected dependency of the bender length. In case of the 2 cm long bender the dose rate is a factor of 2.6 higher and in case of the 20 cm long bender the dose rate is a factor of 2.9 lower than compared with a 10 cm long bender. The small peaks mark the beginning of the bender and are caused by back-scattered particles when the neutrons imping on the Si-bender. However, the radial thickness as well as the axial length of the shielding is not influenced by the bender length. As can be seen in the right picture of Fig. 6 the differences in the dose rate are negligible for more than 0.6 m prependicular to the neutronbeam axis.

6.2 Requiered Length of the Beam Line Shielding

The requiered length to meet the dose rate limit of 0.25 mrem/h was determined by analyzing the spatial distribution of the dose rate in the 3.5°-direction. The resulting isodose plots are shown in Fig. 7 for a 11 m and a 10 m long concrete shielding. The last meter of the shielding is made of normal concrete instead of HD-concrete in order to avoid an influence of the magnetic field at the sample position due to the iron components of the HD-concrete. The calculations show, that length of the shielding up to the beginning of the fourth chopper is sufficient. The analysis of the data showed, that gamma-radiation is a minor contribution to the total dose rate. On the beam axis the dose rate limit is met in a distance

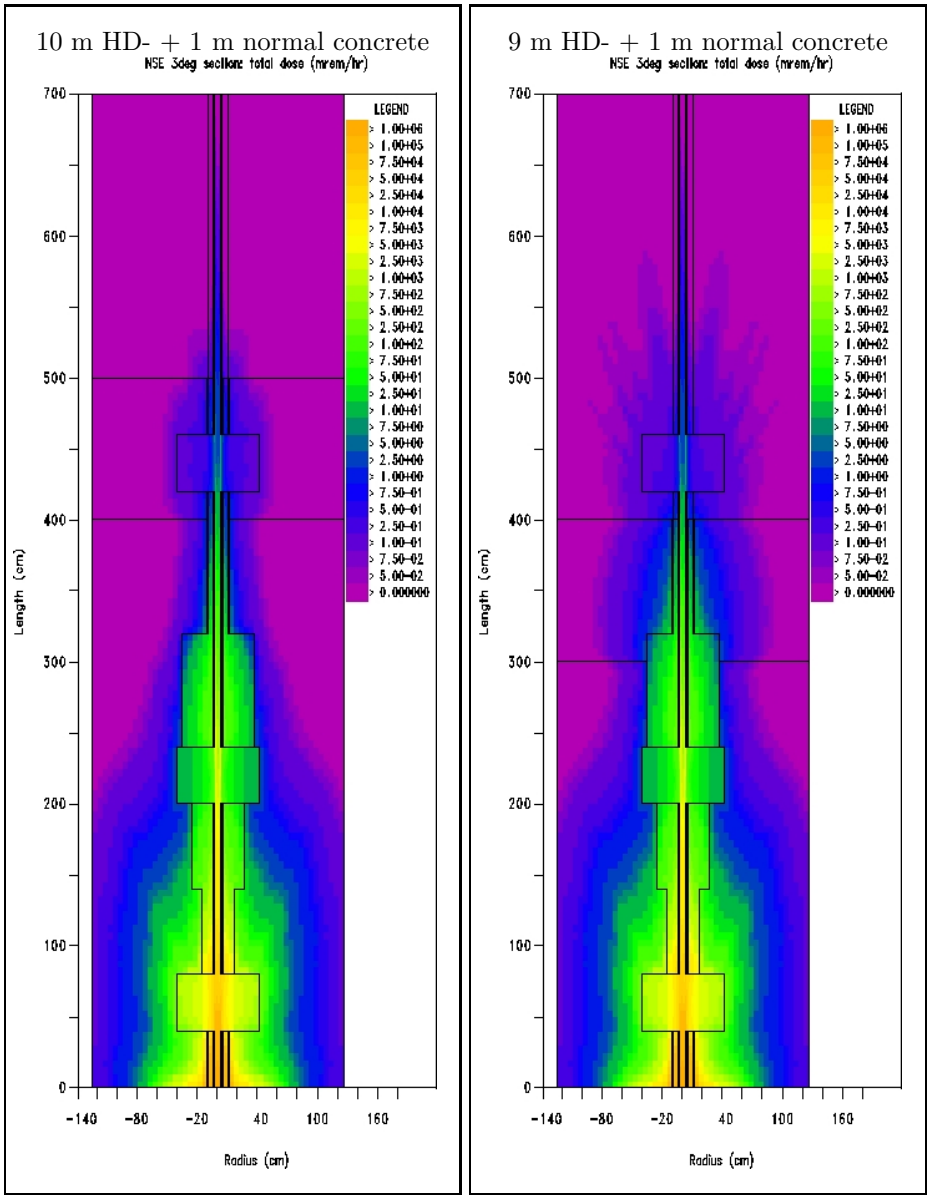

Figure 7: Isodose plots for a 11 m (left picture) and 10 m (right picture) long beamline shielding.

of 12 m from the moderator surface. We like to point out, that the contribution of thermal and cold neutrons, which are transported through the neutron guide is not included in this estimation, because the neutron optical properties of the neutron guide are not included in the applied codes.

6.3 Required Thickness of the Beam Line Shielding

To determine the required thickness of the shielding the distance from the beam axis where the dose rate limit is met was determined as a function from the distance from the moderator surface. Fig. 8 illustrates the results for the 0°-direction and the 3.5°-direction with a stainless steel beamstop. In case of the 0°-direction the dose rate vanished after 9 m due to the stainless steel beamstop. In the 3.5°-direction the dose rate limit can be achieved with the same thickness up 8.5 m than compared to the 0°-direction. For longer distances the dose rate limit is met in a distance of 0.4 m from the beam axis. After 11 m the dose rate requirements outside the neutron beam line are fulfilled without additional shielding material.

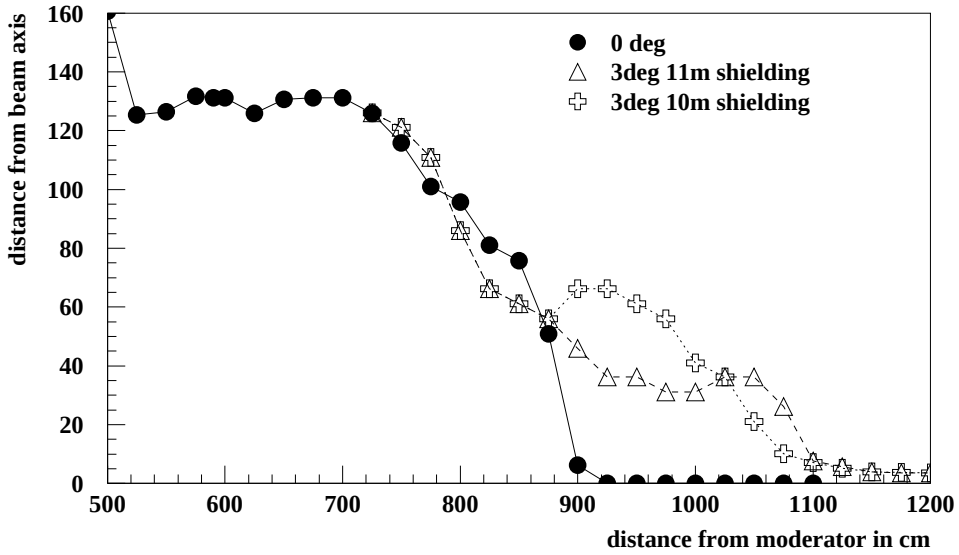

Figure 8: Distance from the beam axis where the dose rate limit of 0.25 mrem/h is met as a function of the beam line length.

6.4 Radial Dependency of the Dose Rate in 3.5°-Direction

In Fig. 9 the dose rate as a function of the radius is shown for four selected axial position: at 6.90 m, 8.90 m, 10.40 m (fourth chopper cavity), and 10.90 m (directly behind the shielding). Further a comparison of a 10 m long and an 11 m long beam line shielding is shown in Fig. 9. For z<9.0 m no influence of the

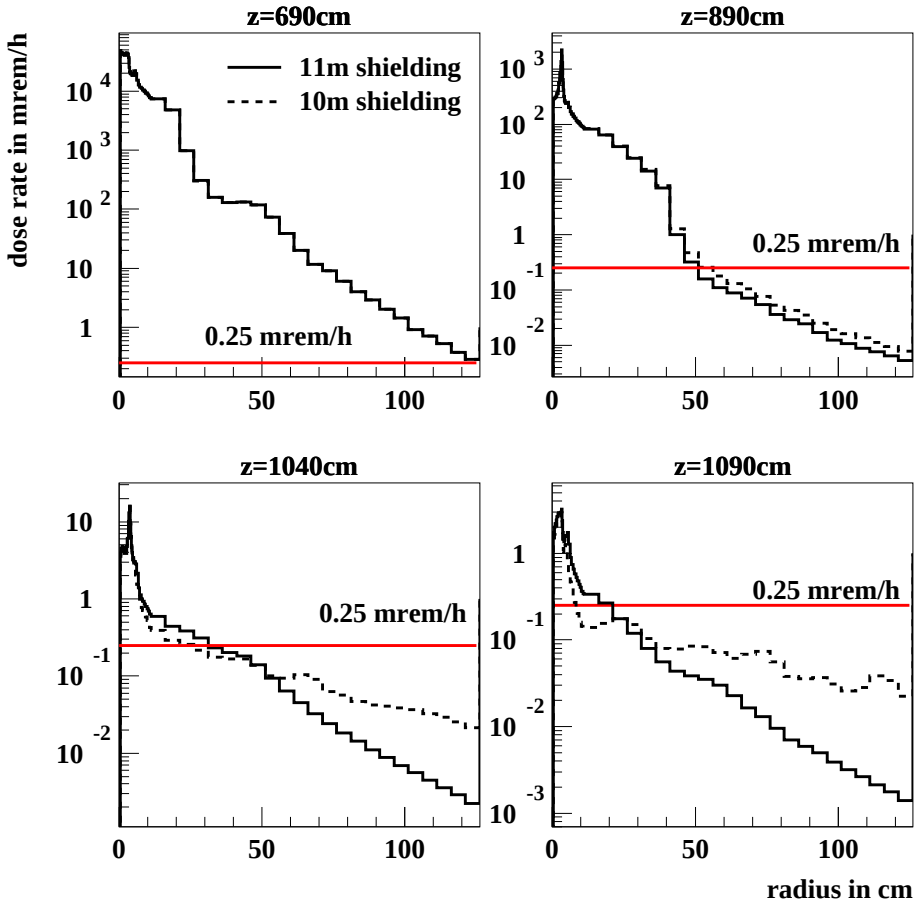

Figure 9: Radial dependency of the dose rate at selected axial positions. The red line marks the dose rate limit of 0.25 mrem/h.

shielding length can be found, because the geometry in the region is the same in both cases. In case of the 10 m long beamline the material changes from HD-concrete to normal concrete at z=9.0 m. For lengths z>10 m there is only air instead of normal concrete –as it is in this region for the 11 m long shielding–resulting in a slighter slope of the histograms for the 10 m long beam line shielding as it can be seen in the histograms for z=10.4 m and 10.9 m. However, the dose rate limit is met in both cases, but the background due to high energy neutrons is one order of magnitude higher, which is more an instrument desing question rather than a radiation protection issue.

7 Energy Dependency

In this section the energy dependency of the dose rate is discussed. The results shown below are for the dose rate behaviour on the neutron beam axis. At first the situation in the 0°-direction will be described. As shown in Fig. 10 the contribution of the different energy regions to the total dose rate changes over

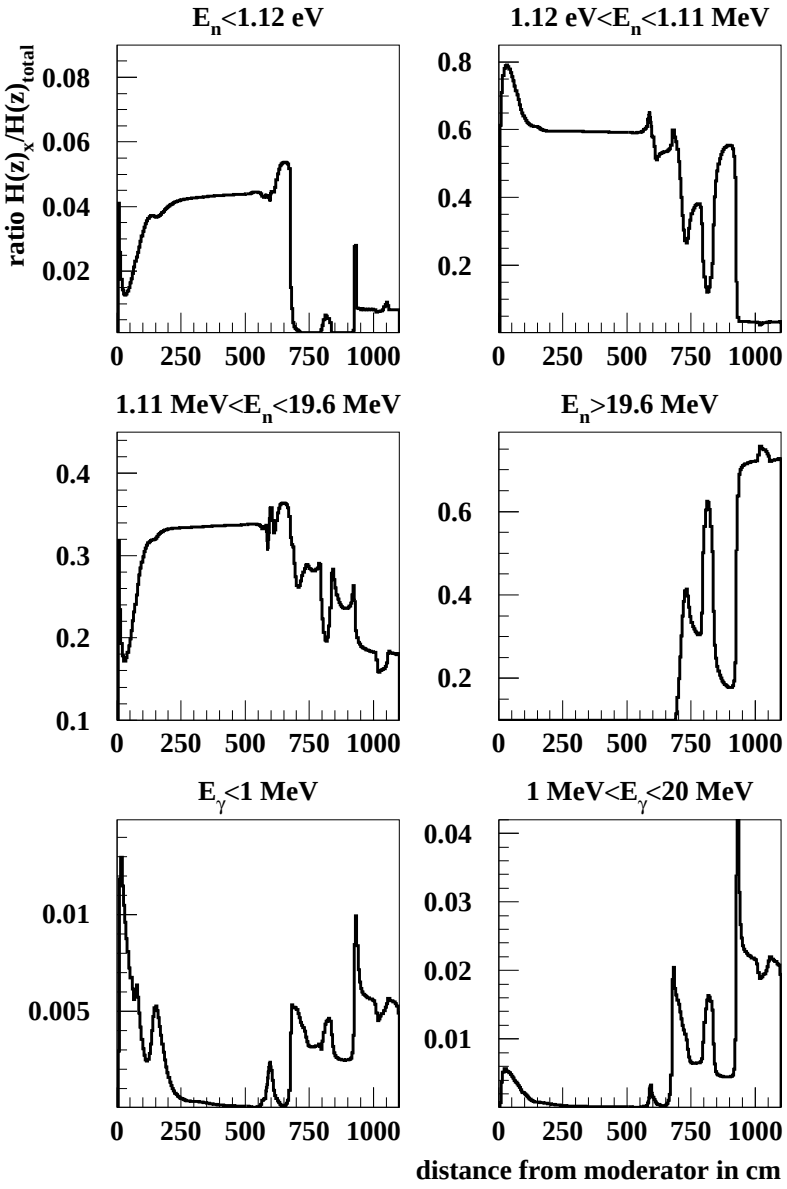

Figure 10: Contribution to the dose rate from different energy regions and particle types as a function of the distance from the moderator in 0°-direction.

the shielding length. Over the first 8 m the epithermal neutrons cause 60 % of the total dose rate. Above 8 m shielding length neutons with a kinetic energy above 19.6 MeV plays the dominant role with a ratio of more than 70 % compared to the total dose rate. The contribution of γ-radiation is negligible with less than 3 %. The same is true for for thermal and cold neutrons with less than 5 %.

The situation in the 3.5°-direction is a different as the histograms in Fig. 11 illustrate. After a distance of 5 m from the midpoint of the bender thermal and epithermal neutrons are negligible. Here, especially neutrons with a kinetic energy above 19.6 MeV are dominant with an amount of more than 70 %.
As already mentioned the amount of thermal and cold neutrons transported through the neutron guide is not included in this calculations.

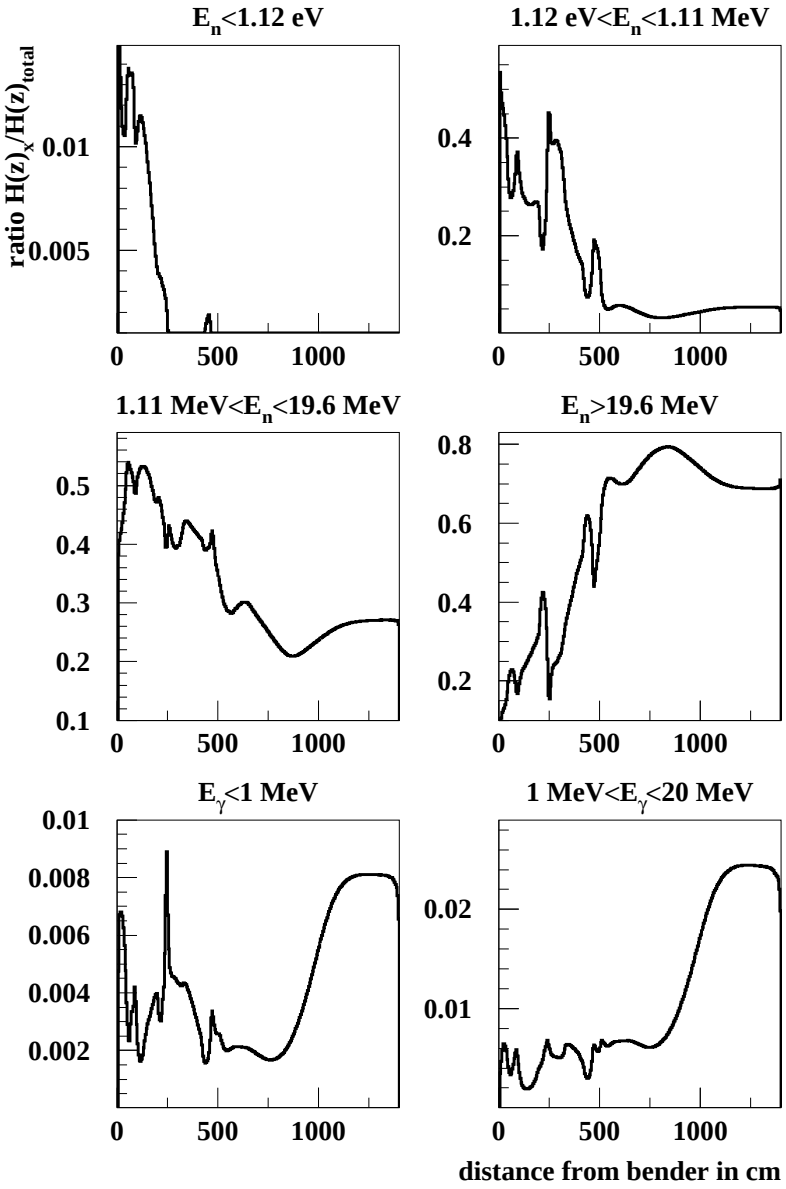

Figure 11: Contribution to the dose rate from different energy regions and particle types as a function of the distance from the moderator in 3.5°-direction.

8 Investigation of Different Beamstop Materials

The materials – HD-concrete, stainless steel, and tungsten– have been investigated as possible beamstop materials. The spatial dose rate distributions for the bended part of the beamline are shown in Fig. 12. It can be seen, that the needed length of the shielding is not influenced by the chosen material. However,

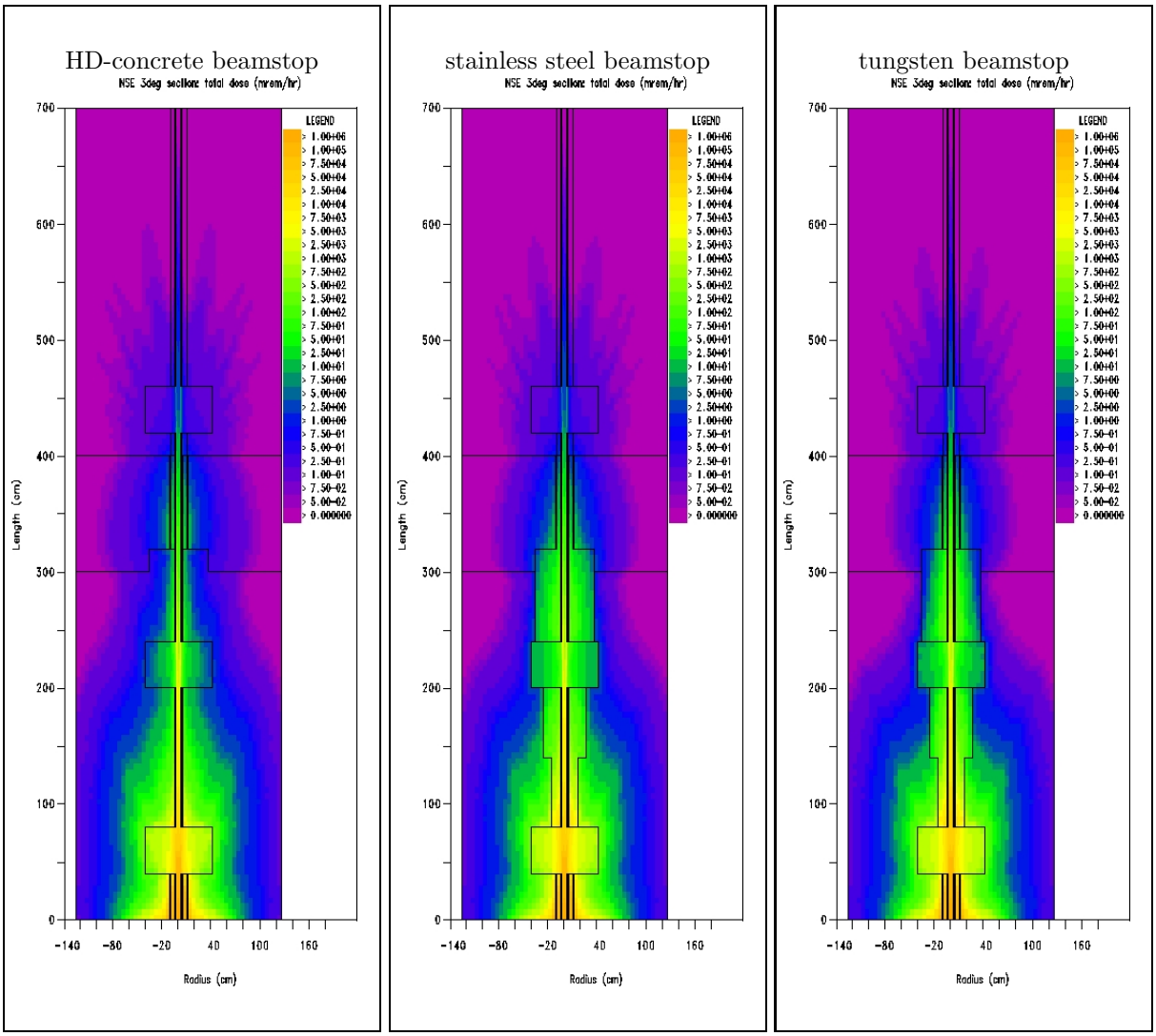

Figure 12: Isodose plots for radiation shielding with a stainless steel beamstop (left picture) and a tungsten ($\rho = 19.3 \frac{g}{cm^2}$) beamstop (right picture).

in radial direction the required thickness of the shielding is slightly influenced. In case of tungsten a thinner radiation shielding is sufficient.

9 A First Engineering Design

From the above descibed results an enginieering desing was developed.

10 Conclusion

First shielding calculations using the DORT code were performed to estimate the expected dose rates for the neutron beam line shielding at beam line 15. The influcence of several shielding materials and beam stop materials was investigated. The results lead to a first rough design of the proposed beam line shielding. In the next step the results of this study will be used as basic parameters for the mechanical design of the shielding. It has to be discussed, if more detailed calculations will be needed. Furthermore the source term has to be discussed because the normalization overestimates the actual beam intensity. The cross talk from adjacent beam lines was not taken into acount.

References

[1] H.G. Hughes et al.,
MCNPX–The LAHET/MCNP Code Merger,
X-Division Research Note XTM-RN(U)97-012, LA-UR-97-4891,
Los Alamos National Laboratory (1997)

[2] W.A. Rhoades and R.L. Childs,
The DORT Two-Dimensional Dicrete Ordinates Transport Code,
Nucl.Sci.&Engr.**99**,1,88-89(May 1988)

[3] R.A. Lillie and F.X. Gallmeier,
Source Terms for all Beam Tube Calculations

[4] R.L. Childs,
GRTUNCL: First Collision Source Program,
RSICC Computer Code Collections, DOORS 3.2,Section 9,July 1998

[5] R.A. Lillie and F.X. Gallmeier,
HILO Transport Cross-Section Library Extension,
Proc. of the 3^{rd} Int. Topical Meeting on Nuclear Applications of Accelerator Technology, pp. 520-526,
American Nuclear Society, La Grange Park, 1999

[6] G.C. Haynes,
The AXMIX Program for Cross Section Mixing and Library Arrangement,
TM-5295, December 1974

[7] W.A. Rhoades,
The GIP Program for Preperation of Group-Organized Cross Section Libraries",
Informal Notes, November 1975

[8] T.M. Miller, R.E. Pevey, R.A. Lillie, and J.O. Johnson,
Radiation Transport Analysis in Support of the SNS Target Station Neutron Beamline Shutters Title I Design,
SNS 106100200-TR0048-R00, September 2000